JACS
JOURNAL OF THE AMERICAN CHEMICAL SOCIETY

Article

Positional Selectivity in C–H Functionalizations of 2-Benzyl Furans with Bimetallic Catalysts

Jiadi Zhang, Sheng-Chun Sha, Ana Bellomo, Nisalak Trongsiriwat, Feng Gao, Neil C. Tomson, and Patrick J Walsh

J. Am. Chem. Soc., **Just Accepted Manuscript** • DOI: 10.1021/jacs.6b01578 • Publication Date (Web): 03 Mar 2016

Just Accepted

ACS Publications

Journal of the American Chemical Society is published by the American Chemical Society. 1155 Sixteenth Street N.W., Washington, DC 20036

Positional Selectivity in C–H Functionalizations of 2-Benzyl Furans with Bimetallic Catalysts

Jiadi Zhang, Sheng-Chun Sha, Ana Bellomo, Nisalak Trongsiriwat, Feng Gao, Neil C. Tomson,* and Patrick J. Walsh*

Roy and Diana Vagelos Laboratories, Penn/Merck Laboratory for High-Throughput Experimentation, Department of Chemistry, University of Pennsylvania, 231 South 34th Street, Philadelphia, Pennsylvania 19104-6323, United States

Supporting Information Placeholder

ABSTRACT: Metal-catalyzed carbon-carbon bond-forming reactions are a mainstay in the synthesis of pharmaceutical agents. A long-standing problem plaguing the field of transition metal catalyzed C–H functionalization chemistry is control of selectivity among inequivalent C–H bonds in organic reactants. Herein we advance an approach to direct site selectivity in the arylation of 2-benzyl furans founded on the idea that modulation of cooperativity in bimetallic catalysts can enable navigation of selectivity. The bimetallic catalysts introduced herein exert a high degree of control, leading to divergent site-selective arylation reactions of both sp^2 and sp^3 C–H bonds of 2-benzyl furans. It is proposed that the selectivity is govern by cation-π interactions, which can be modulated by choice of base and accompanying additives [$MN(SiMe_3)_2$, M = K or Li•12-crown-4].

1. INTRODUCTION

Recent years have witnessed spectacular advances in transition metal catalyzed C–H functionalization reactions,[1-7] which have numerous potential applications in the synthesis of biologically active compounds and pharmaceuticals.[8,9] Despite remarkable progress, a central challenge remains achievement of positional selectivity in the presence of inequivalent C–H bonds.[10] One strategy to approach this problem is the installation of directing groups that position the catalyst to react selectively with the C–H bond of interest,[11-14] through either oxidative addition or other means of activation. This strategy is particularly useful when the directing group is part of the target molecule, or is readily removed.

An alternative approach is to exert control over the *reductive elimination step* of a C–H functionalization reaction. Doing so would require a directing group to influence the equilibrium between various organometallic isomers. We hypothesized that use of bimetallic catalysts could provide unique opportunities to enhance catalyst selectivity beyond that obtainable by the mononuclear catalysts that are the state-of-the-art in coupling reactions.

Inspiration for this mode of regiochemical control came from the synergistic reactivity we observed of a heterobimetallic Pd/M catalyst (M=Li, Na, K)[15] based on the NIXANTPHOS[16] scaffolding (Figure 1). This catalyst exhibits much greater reactivity in the oxidative addition of aryl chlorides than the most reactive bidentate phosphine complexes of palladium known to catalyze cross-coupling reactions. Importantly, the (NIXANTPHOS)Pd complex's N–H must be deprotonated to generate the active bimetallic catalyst that achieves the room temperature oxidative addition of aryl chlorides.[15] For the purposes of directing C–H functionalization reactions at the reductive elimination step, we envision using the cooperativity between proximate metallic sites in bimetallic catalysts.[17,18] Not only could the presence of a second metal ion engender the types of novel reactivity observed during Ar–Cl activation, but we thought that variation of the identity of the auxiliary metal could also impart divergent reaction pathways, as depicted in Figure 2.

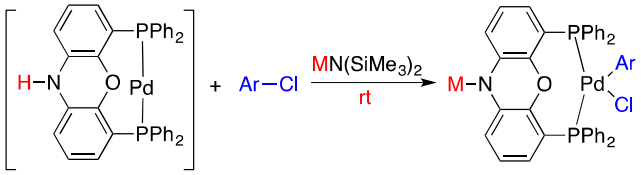

(NIXANTPHOS)Pd(0)

Figure 1. Oxidative addition of aryl chlorides by deprotonated (NIXANTPHOS)Pd(0).

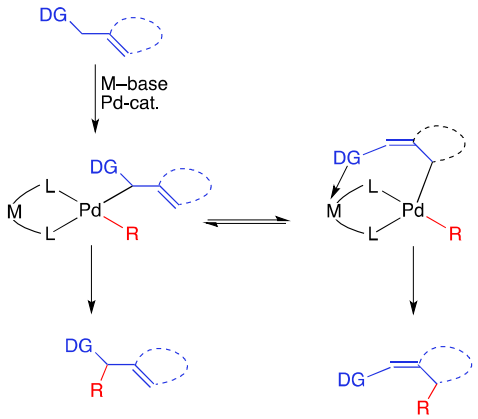

Figure 2. Cooperativity in heterobimetallic catalysts via directing group to control regioselectivity in reductive elimination.

Herein, we advance room temperature site-selective arylation reactions at both sp^2 and sp^3 hybridized carbons with bimetallic catalysts employing 2-benzyl furan derivatives (Figure 3). Nearly complete selectivity is reached in the reductive elimination between the two reaction pathways under conditions that differ *only in the nature of the auxiliary metal and its accompanying ligands*. These divergent routes provide access to differentially substituted furans, a class of heterocycles ubiquitous in naturally occurring and biologically active compounds.[19,20] Experimental and computational studies support cation-π

interactions as the controlling feature enabling the regioselective C-3 arylation of 2-benzyl furans.

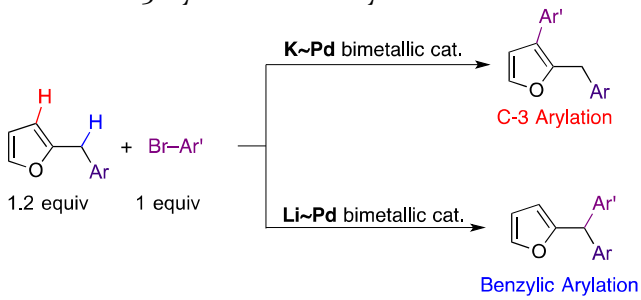

Figure 3. Cation-controlled site-selective sp^2 C-3–H and sp^3 benzylic C–H arylation of furans

2. RESULTS AND DISCUSSION

2.1. Initial Studies with 2-Benzylfuran.

In our search for substrates to probe cooperativity in reductive elimination from bimetallic catalysts, we discovered that 2-benzyl furans gave mixtures of products derived from C-3 and benzylic arylation reactions (Figure 3). We, therefore, initiated an exploration of site-selectivity in the arylation of 2-benzylfuran (**1a**) using NIXANTPHOS (structure in Figure 1), $Pd(OAc)_2$, base, and 4-*tert*-butyl bromobenzene (**2b**). Given the high pK_a of the benzylic C–H's of 2-benzylfuran (30.2 in DMSO),[21] we chose $KN(SiMe_3)_2$ as a starting point. Selected results are shown in Table 1 (with details in the Supporting Information).

To favor the unusual C-3 arylation product (**3ab**), 4 ethereal solvents [CPME (cyclopentyl methyl ether), dioxane, THF, and 2-MeTHF] were tested under otherwise identical conditions (see SI for details). Among the four solvents, dioxane proved to be the best. Using 2.5 equivalents $KN(SiMe_3)_2$ resulted in 93% assay yield (AY by ^{1}H NMR) of C-3 arylation with a >14:1 ratio of **3ab** : the diarylation product **4ab** (entry 1). The C-3 arylation product was ultimately isolated in 93% yield after flash chromatography.

Table 1. Optimization of Pd-catalyzed C-3 and benzylic arylation of **1a**[a]

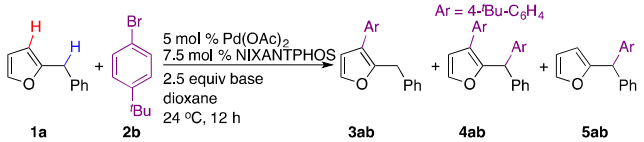

entry	base	3ab (%)[a]	4ab (%)[a]	5ab (%)[a]
1	$KN(SiMe_3)_2$	93(93)[b]	6	0
2	$NaN(SiMe_3)_2$	<5	<5	29
3	$LiN(SiMe_3)_2$	0	0	0
4	$KN(SiMe_3)_2$:18-crown-6[c]	0	13	51
5	$NaN(SiMe_3)_2$:15-crown-5[c]	0	<5	39
6	$LiN(SiMe_3)_2$:12-crown-4[c]	0	0	94(91)[b]

[a]Yield determined by ^{1}H NMR spectroscopy of the crude reaction mixture. [b]Isolated yield after chromatographic purification. [c]Crown ether (2 equiv relative to base) employed.

We next explored the impact of different bases on the selectivity of the heterobimetallic catalyst. Substitution of $NaN(SiMe_3)_2$ for $KN(SiMe_3)_2$ under otherwise identical conditions resulted in a remarkable change in the course of the reaction, generating benzylic arylation (**5ab**) with high selectivity, albeit in 29% AY (entry 2). Based on our prior results,[22] we were not surprised that $LiN(SiMe_3)_2$ was not sufficiently reactive to deprotonate the weakly acidic substrate, and no reaction was observed (entry 3). We previously demonstrated that additives that bind to M of $MN(SiMe_3)_2$ (M = Li, Na) accelerate the *deprotonation step* of deprotonative cross-coupling processes (DCCP), presumably by reducing the aggregation state of the base.[22] Crown ethers were found to exhibit the greatest acceleration. Thus, we explored the use of 2 equiv of the corresponding crown ethers relative to base (entries 4–6). Interestingly, addition of 12-crown-4 (5 equiv) to the reaction with $LiN(SiMe_3)_2$ afforded the benzylic arylation product **5ab** *exclusively* in 94% AY and 91% isolated yield. The impact of 15-crown-5 on the reaction with $NaN(SiMe_3)_2$ was to increase the yield of the benzylic arylation product (entry 5). Importantly, and in sharp contrast to the use of $KN(SiMe_3)_2$ alone, the potassium cation caged with 18-crown-6 (1:2) afforded the *benzylic arylation product* ***5ab*** as the major product without formation of the C-3 arylation product **3ab** (entry 1 vs. 6). It is noteworthy that no reaction was observed in the absence of NIXANTPHOS. The implications of the results in Table 1 and investigation of the factors controlling selectivity are discussed in the next sections.

2.2. Probing the Divergent Reaction Pathways Leading to C-3 and Benzylic Arylation.

To rationalize the formation of the C-3 arylation product, we propose the reaction pathway in Figure 4.[23,24] Reversible deprotonation of the substrate by $MN(SiMe_3)_2$ (M = Li, Na, K) forms the carbanion (**I**), which undergoes transmetallation to the Ar–Br oxidative addition product **II** to give benzyl adduct **III**. Reductive elimination at this point would generate the C_{Bn}-arylation product **VIII**, but intermediate **III** is in equilibrium with the C-3 adduct **IV** via a σ–π–σ rearrangement. Reductive elimination of the C-3 adduct **IV** and subsequent tautomerization of **V** generates the C-3 arylation product (**VI**). As mentioned above, by changing $MN(SiMe_3)_2$ bases and thereby also changing the auxiliary metal (Figure 4), we proposed that we could impact the bifurcation between the C-3 and benzylic arylation reaction manifolds at the reductive elimination step (as detailed below).

The results in Table 1 provide critical insight into the function of our bimetallic catalysts and lead us to hypothesize that when the NIXANTPHOS-bound potassium has available coordination sites, it binds the phenyl group of the substrate forcing palladium to bind at C-3. In contrast, when the potassium is caged by the crown ether it is coordinatively saturated and unable to bind the phenyl of the substrate. As a result, palladium binds and arylates the benzylic site. Although cation-π interactions have been studied in water,[25] less is known about the strength

of such interactions relative to solvent binding in different organic solvents. Thus, the key to controlling C-3 vs. benzylic selectivity in this bimetallic catalyst is the ability to switch on and off cooperativity between the auxiliary metal and the palladium. It is noteworthy that directed C–H functionalization reactions that occur in the second coordination sphere are rare,[14] let alone those that involve cation-π interactions.

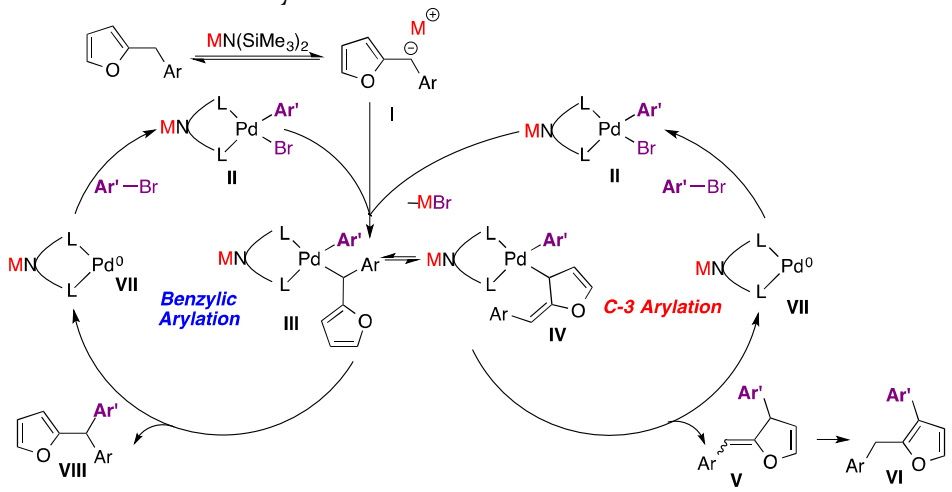

Figure 4. Proposed reaction pathways for benzylic and C-3 arylations

2.3 Computational Exploration of Arylation Regioselectivity.

Computational chemistry was used to help understand the factors that control the bifurcation of the arylation reaction pathways. To start, density functional theory geometry optimization calculations (BP86/ZORA-TZVP, COSMO[dioxane]; see Supplementary Information) were performed on model compounds of intermediates **III** and **IV** (Figure 4). Comparison of the Pd–C_{Bn} ($[\mathbf{III}]^-$) and Pd–C-3 ($[\mathbf{IV}]^-$) tautomers of the anion [(NIXANTPHOS)Pd(Ph)(2-benzylfuranyl)]$^-$ (no auxiliary metal; Figure 5, top) revealed a 5.0 kcal/mol preference for the Pd–C_{Bn} bond (Figure 6), in line with the observation that caging the K auxiliary metal with crown ether additive favors benzylic arylation products.

The geometries about the metal centers of $[\mathbf{III}]^-$ and $[\mathbf{IV}]^-$ are both pseudo square planar, with pairs of nearly *trans*-disposed phosphines (∠(P–Pd–P) = 142°) and carbons (∠(C–Pd–C) = 160°). Long Pd–O distances of *ca.* 2.8 Å lie well outside the sum of the covalent radii of Pd and O (2.05 Å).[26] The Pd–C(47) ($[\mathbf{III}]^-$) and Pd–C(1) ($[\mathbf{IV}]^-$) bond distances of 2.236 and 2.296 Å, respectively, notably also lie outside the 2.15 Å sum of the covalent radii of Pd and C and are considerably longer than the Pd–C(26) bond lengths of *ca.* 2.08 Å. We attribute the weakness of Pd–$C_{substrate}$ interactions to the resonance stabilization of the anions that would result from heterolytic dissociation.

A series of solvated non-ionic K-NIXANTPHOS complexes were next used to explore the C-3 arylation product. We hypothesized that a cation–π interaction was instrumental in determining the observed regioselectivity, but for this to be the case, the K–arene interaction would have to outcompete solvation by dioxane. To investigate this computationally, we used the conductor-like screening model (COSMO) as implemented in ORCA, with the dielectric constant of dioxane. We then manually investigated the explicit solvation sphere of the complex by comparing the energies of various geometries of $\mathbf{K[III]\cdot(diox)_4}$, $\mathbf{K[IV]\cdot(diox)_4}$, and {$\mathbf{K[IV]\cdot(diox)_3}$ + dioxane}. In line with the relative energies of $[\mathbf{III}]^-$ and $[\mathbf{IV}]^-$ given above, $\mathbf{K[III]\cdot(diox)_4}$ was found to be more stable than $\mathbf{K[IV]\cdot(diox)_4}$, albeit by only 1.3 kcal/mol (Figure 6). However, dissociation of a dioxane from $\mathbf{K[IV]\cdot(diox)_4}$ provided a substantial entropic gain of 12.4 kcal/mol in free energy. Thus, $\mathbf{K[IV]\cdot(diox)_3}$ (Figure 6, bottom) plus a free molecule of dioxane was determined to be the ground state of the system, with a clear energetic separation between it and the next lowest energy conformation ($\mathbf{K[III]\cdot(diox)_4}$, +11.1 kcal/mol, Figure 6).

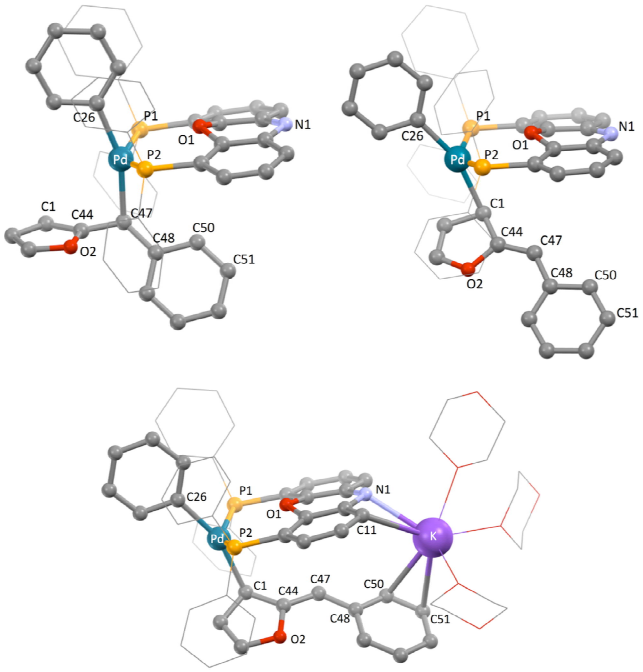

Figure 5. DFT geometry optimized structures of [(NIXANTPHOS)Pd(Ph)(6-Pd-2-benzylfuranyl)]$^-$ (**[III]**$^-$, top left), [(NIXANTPHOS)Pd(Ph)(3-Pd-2-benzylfuranyl)]$^-$ (**[IV]**$^-$, top right) and [K(diox)$_3$][(NIXANTPHOS)Pd(Ph)(3-Pd-2-benzylfuranyl)] (**K[IV]•(diox)$_3$**, bottom); all hydrogen atoms were removed for clarity. Important bond lengths (Å) and angles (°) for *i*) **[III]**$^-$: Pd–C47 2.236, Pd–C26 2.085, Pd–P1 2.398, Pd–P2 2.401, C44–C47 1.459, P1–Pd–P2 142.1, C26–Pd–C47 159.6; *ii*) **[IV]**$^-$: Pd–C1 2.296, Pd–C26 2.076, Pd–P1 2.417, Pd–P2 2.358, C44–C47 1.373, P1–Pd–P2 141.8, C26–Pd–C47 160.6; and **K[IV]•(diox)$_3$**: Pd–C1 2.301, Pd–C26 2.072, K–N 2.828, K–C50 3.430, K–C51 3.384, P1–Pd–P2 145.0, C1–Pd–C26 158.4.

The most notable structural feature of **K[IV]•(diox)$_3$** is the cation–π interaction[27,28] between potassium and the substrate arene ring (K–C$_\pi$ = 3.384, 3.430 Å; Figure 5, bottom). The greater polarizability of K$^+$ compared to the lighter alkali metals is well known to facilitate cation-π interactions,[27,28] and it is proposed this interaction may be strong enough to perturb the equilibrium between Pd–C(3) and Pd–C$_{Bn}$ intermediates **III** and **IV** (Figure 4), guiding reductive elimination in the direction of the observed C-3 arylation product.

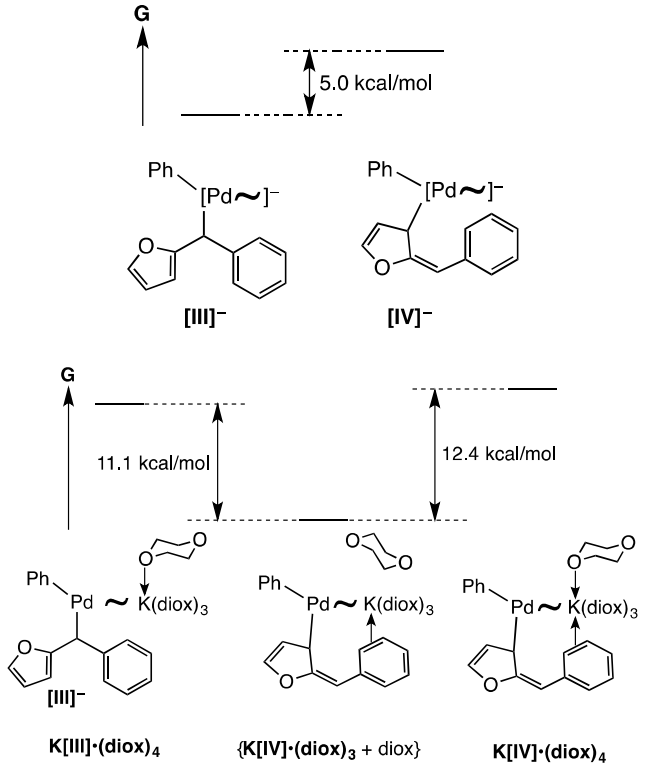

Figure 6. Graphical description of the energy differences between *i*) **[III]**$^-$ and **[IV]**$^-$ (left) and *ii*) **K[III]•(diox)$_4$** and **K[IV]•(diox)$_3$** + dioxane. The tilde symbol represents the deprotonated NIXANTPHOS ligand.

Analogous computations on the Na complexes of **[III]**$^-$ and **[IV]**$^-$ found the di-solvate [Na(dioxane)$_2$][(NIXANTPHOS)Pd(Ph)(3-Pd-2-benzylfuranyl)] (**Na[IV]•(diox)$_2$**) plus free dioxane to lie 5.5 kcal/mol lower in energy than the Pd–C$_{Bn}$ tri-solvate **Na[III]•(diox)$_3$** and 11.4 kcal/mol lower in energy than the tri-solvate of the Pd–C(3) tautomer, **Na[IV]•(diox)$_3$** (see Supporting Information). **Na[IV]•(diox)$_2$** similarly displays a cation–π interaction, with short Na–C$_\pi$ distances of 2.815 and 2.948 Å. The trend toward a smaller cation–π stabilization energy is consistent with the diminished capacity of the harder metal ion to form cation–π interactions capable of outcompeting solvation.

2.4 Generality of Aryl Bromides in M~Pd(NIXANTPHOS)-Catalyzed C-3 and Benzylic Arylations of 1.

We next desired to probe whether the site-selectivity could be influenced by the steric and/or electronic properties of the substrates, first using different aryl bromides. As detailed below, the nature of the coupling partner had little effect on the reaction outcome, enabling the synthesis of an array of C-3 arylated furans **3aa**–**3gb** from sterically and electronically diverse aryl and heteroaryl bromides. As outlined in Table 2, employing KN(SiMe$_3$)$_2$ as base led to excellent C-3 selectivity with no benzylic arylation products **5** observed (^{1}H NMR spectroscopy). Good to excellent selectivity for mono- over diarylation was also exhibited (C-3:diarylation from 5:1 to > 20:1). All the C-3 arylation products were easily separable from the diarylation byproducts by column chromatography, delivering **3aa**–**3gb** in 27–99% isolated yields. Excellent yields were obtained using bromobenzene (**2a**) and aryl bromides bearing 4-alkyl (**2b**), 4-methoxy (**2c**), 4-*N*,*N*-dimethylamino (**2d**) as well as 4-fluoro (**2e**) groups, all with C-3:diarylation ratios ≥ 11:1. 1-Bromo-4-chlorobenzene (**2f**) reacted with **1a** to produce C-3 arylation product **3af** in 55% isolated yield with the C-3:diarylation ratio of 13:1. Trifluoromethyl (**2g**), methoxy (**2h**), and acetal (**2i**) groups at the *meta* position were all well-tolerated (65–77% yields) with moderate to good C-3:diarylation ratios (≥ 5:1). The sterically hindered 1-bromonaphthalene (**2j**) and 2-bromotoluene (**2k**) also participated in C-3 arylation to produce **3aj** and **3ak** with C-3:diarylation ratios > 20:1. Aryl bromides containing an acetyl (**2l**) and heterocycles such as benzofuran (**2m**) and indole (**2n**, **2o**) exhibited excellent C-3:diarylation ratios (> 20:1), delivering the desired products in 56–80% yields. Combined with the analogous results given below for varying the identity of **2** under C$_{Bn}$-arylation conditions, these results suggest that site-selectivity is not being determined by aryl bromide substrate.

A similar result was found when we examined the impact of substituents on the aryl group of the 2-benzylfuran. The parent phenyl (**1a**) and 4-fluoro phenyl (**1b**) substrates were able to deliver the C-3 arylation products **3ab** and **3bb** in excellent yields and C-3:diarylation ratios. Still, the 4-methoxy derivative (**1c**) gave only 27% AY of **3cb** (^{1}H NMR spectroscopy) with the C-3:diarylation ratio of 1:1 when 4-*tert*-butyl bromobenzene was employed. This result suggests that half of the initial C-3 arylation product **3cb** underwent a second ary-

lation to form the diarylation byproduct **4cb**, because the rates of these arylation processes are similar. We hypothesized that the 4-methoxy benzyl group of **1c** decreased the acidity of the benzylic hydrogens (relative to **1a** and **1b**), slowing the rate of the C-3 arylation. Once arylated at C-3, however, the impact of the C-3 aryl is to increase the acidity of the benzylic hydrogens and, therefore, the relative rate of arylation of the benzylic position to generate the diarylated product. To probe this hypothesis, arylation of **1c** was performed with 4-bromoanisole and 4-bromo-*N,N*-dimethylaniline, respectively. The C-3 arylation intermediate with the dimethyl amino group possesses less acidic benzylic hydrogens, and the relative rate of the C-3 arylation to benzylic arylation is expected to be larger. Consistent with this hypothesis, use of 4-bromo-*N,N*-dimethylaniline resulted in a 57% yield of the C-3 arylation product with a C-3:diarylation ratio of 5:1 (See Supporting Information for more details). Use of 4-bromoanisole gave intermediate results, as predicted (**3cc**, 43% yield).

Cation-π interactions will likely be impacted by the electronic and steric properties of the π-donor. We hypothesized that the reduced electron density in the aryl ring of the electron-deficient 3,5-C_6H_3-$(CF_3)_2$ group of **1d** would render cation-π interactions less favorable. Subjecting benzylic furan **1d** to the C-3 arylation conditions (M = K)[29] resulted in a switch in the C-3 : benzylic arylation ratio to 1.0 : 1.4; *i.e.* the *minor* product was C-3 arylation and the major product was benzylic arylation. Computationally, we found that the Pd–C_{Bn} tautomer of the alkali metal-free anion [(NIXANTPHOS)Pd(Ph)(3-Pd-2-(3,5-$(CF_3)_2$-benzyl)furanyl)]$^-$ ([**III^{CF3}**]$^-$) was computed to lie lower in energy than its Pd–C-3 tautomer ([**IV^{CF3}**]$^-$) by 2.9 kcal/mol. However, in contrast to the parent substrate discussed above, the preference for Pd–C_{Bn} bonding for the fluorinated substrate carries over to the K complexes, where the Pd-C_{Bn} species **K[III^{CF3}]•(diox)$_3$** was found to lie 5.9 kcal/mol lower than the combined energies of **K[IV^{CF3}]•(diox)$_2$** and free dioxane. This is consistent with the return to majority benzylic-arylation product with **1d** (C-3:C_{Bn} = 1.0:1.4), which tracks with the diminished nucleophilicity of the trifluoromethylated arene ring, leading to a product distribution weighted more heavily by the energy of the Pd–C bond than by the K–arene interaction.

Next we attempted to perturb the equilibrium between **III** and **IV** through steric influences. Use of 3,5-^{t}Bu$_2$-benzylfuran as a substrate provided the C3-arylated product in 70% yield under the C3-arylation conditions, suggesting that the increased steric influence of the ^{t}Bu groups has a negligible effect on the C-3/C_{Bn}-arylation regiochemistry. Computation of the proposed intermediate [K(diox)][(NIXANTPHOS)Pd(Ph)(3-Pd-2-(3,5-^{t}Bu$_2$-benzyl)furanyl)] (**K[IV^{tBu}]•diox**; Figure 7) indicates a nearly symmetric cation–π interaction with short K–C_π distances, ranging from 3.14–3.43 Å. Related *meta*-^{t}Bu$_2$-arene potassium-π interactions are known,[30–34] suggesting that the ^{t}Bu groups are not sterically imposing enough to prevent the formation of cation-π interactions, as may be needed to observe the benzylic-arylation product under these conditions. Indeed, it appears that the primary influence of the ^{t}Bu groups is to prevent solvation of the cation, leading to a K–arene complex that is considerably more stable than the higher solvate. These results are again consistent with the notion that cation-π interactions perturb the equilibrium between intermediates **III** and **IV**, away from the benzylic position that would be favored under cation-free conditions and toward the furanyl C3-position.

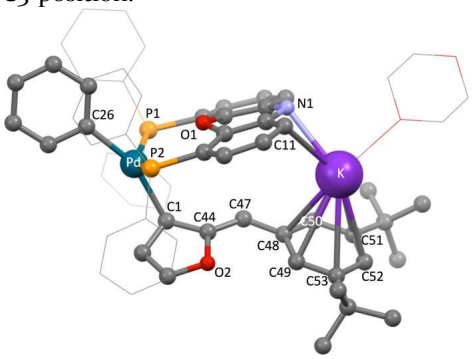

Figure 7. DFT geometry optimized structure of **K[IV^{tBu}]•diox**; all hydrogen atoms were removed for clarity. Important bond lengths (Å) and angles (°): Pd–C1 2.322, Pd–C26 2.067, K–N 2.839, K–C48 3.180, K–C50 3.141, K–C51 3.285, K–C52 3.398, K–C53 3.430, K–C49 3.298, P1–Pd–P2 145.0, C1–Pd–C26 159.4.

Finally, we subjected 2-benzyl-5-methylfuran (**1f**), bearing a C-5 methyl, to the $KN(SiMe_3)_2$ and obtained the C-3 arylation product **3fb** with excellent site selectivity in 70% yield. C-3 arylation of 2-benzhydrylfuran (**1g**, R^1 = 5-CH_3, R^2 = R^3 = Ph) proceeded smoothly in the presence of $KN(SiMe_3)_2$ to afford **3gb** in 99% isolated yield.

Table 2. Scope of aryl bromides in K~Pd(NIXANTPHOS)-catalyzed C-3 arylation of **1a** and derivatives[a]

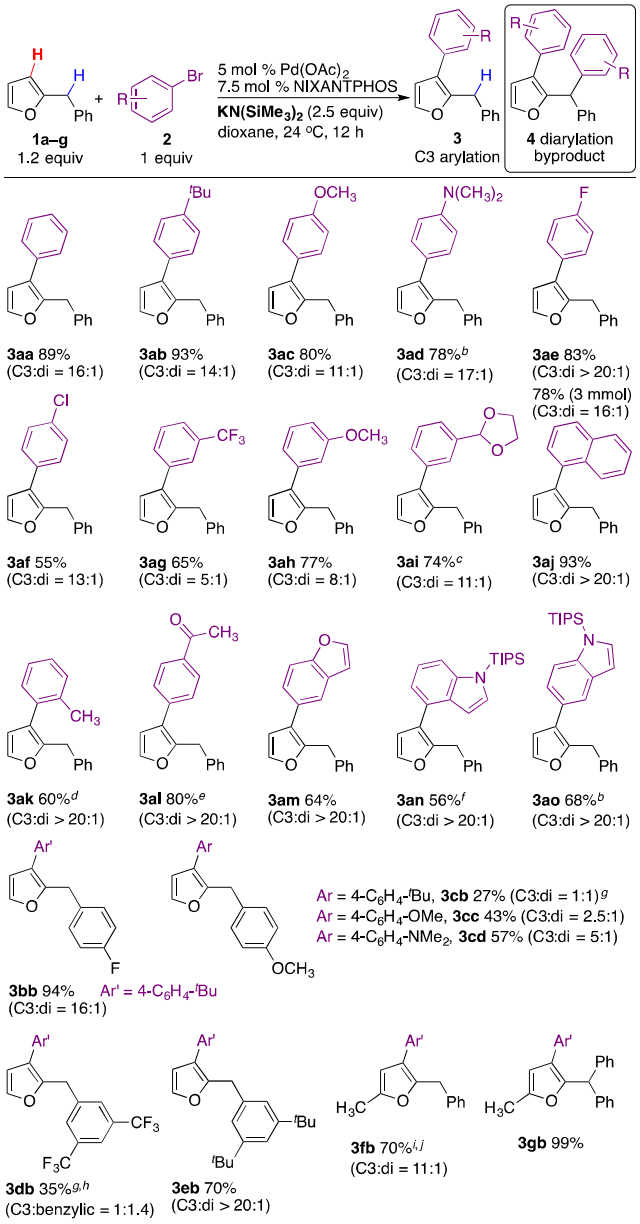

[a]Reactions conducted on a 0.1 mmol scale using 1.2 equiv of **1**, 2.5 equiv of $KN(SiMe_3)_2$, and 1 equiv of **2** at 0.1 M. Isolated yield after chromatographic purification. The C-3:diarylation ratios in parentheses were determined by ^1H NMR spectroscopy of the crude reaction mixtures. [b]45 °C. [c]2 equiv of $KN(SiMe_3)_2$. [d]Reaction conducted on a 0.3 mmol scale. [e]3 equiv of $KN(SiMe_3)_2$. [f]10 mol % $Pd(OAc)_2$ and 15 mol % NIXANTPHOS. [g]Yield determined by ^1H NMR spectroscopy of the crude reaction mixtures. [h]KO^{t}Bu was used as base. [i]2.5 equiv of **1f**. [j]CPME was used as solvent.

To reverse the chemoselectivity, we next employed $LiN(SiMe_3)_2$ with 12-crown-4 (1:2) and determined the generality of aryl bromides in the benzylic arylation of **1a**. As shown in Table 3, with the same aryl bromides employed in the C-3 arylation, a *complete reversal in selectivity towards benzylic arylation was observed*. Neither C-3 arylation nor diarylation products were detected, rendering the exclusive formation of **5** in 60–96% yields. Aryl bromides bearing 4-alkyl (**2b**), electron-donating 4-methoxy (**2c**) and 4-*N*,*N*-dimethylamino (**2d**), 4-fluoro (**2e**) as well as sterically more hindered 1-naphthyl (**2j**) groups all proved to be good cross-coupling partners for the benzylic arylation. Furthermore, functional groups such as acetal (**2i**), acetyl (**2l**) and heterocycles such as benzofuran (**2m**) and indole (**2n**, **2o**) were well tolerated, delivering the corresponding products in 60–96% yields.

The impact of the furan substrate in the benzylic arylations was next explored with 4-*tert*-butyl bromobenzene **2b**. In the presence of $LiN(SiMe_3)_2$ with 12-crown-4 only benzylic arylation products **5** were observed (Table 3, last row). Varying the substituents on the furanyl phenyl group from H (**1a**) to 4-F (**1b**), 4-OCH_3 (**1c**), and 3,5-$(CF_3)_2$ (**1d**) resulted in excellent isolated yields of the benzylic arylation products (75–91%), suggesting that these 4 substrates were reversibly deprotonated and entered the catalytic cycle. Note, however, that with the 3,5-$(CF_3)_2$ (**1d**), decomposition was observed with $LiN(SiMe_3)_2$ and that use of NaO^{t}Bu gave benzylic arylation (85% yield). Subjecting 2-benzyl-5-methylfuran (**1f**), bearing a C-5 methyl, to the $LiN(SiMe_3)_2$ and 12-crown-4 reaction conditions resulted in benzylic arylation product with excellent site selectivity in 94% yield.

Table 3. Scope of aryl bromides in (crown)Li~Pd(NIXANTPHOS)-catalyzed benzylic arylation of **1a** and derivatives [a]

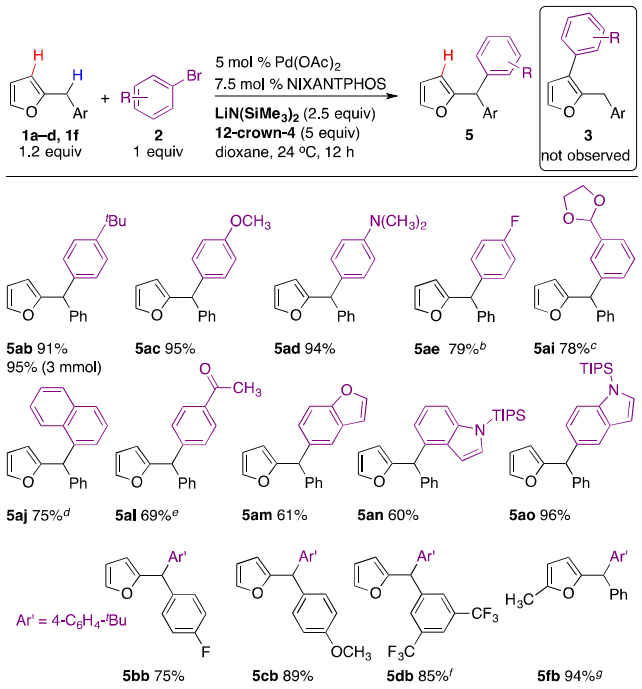

[a]Reactions conducted on a 0.1 mmol scale using 1.2 equiv of **1**, 2.5 equiv of $LiN(SiMe_3)_2$, 5 equiv of 12-crown-4, and 1 equiv of **2** at 0.1 M. Isolated yield after chromatographic purification. [b]**1a**:$LiN(SiMe_3)_2$:12-crown-4:**2** = 2:1.5:3:1. [c]**1a**:$LiN(SiMe_3)_2$:12-crown-4:**2** = 2:2:4:1. [d]**1a**:$LiN(SiMe_3)_2$:12-crown-4:**2** = 1:2:4:2. [e]**1a**:$LiN(SiMe_3)_2$:12-crown-4:**2** = 1.2:3:6:1. [f]NaO^{t}Bu was used as base. [g]CPME was used as solvent.

3. SUMMARY AND OUTLOOK

Nature has long recognized that the placement of two or more metals in close proximity can elicit unique reactivity, as demonstrated by its use of bimetallic enzyme cofactors in various processes (i.e., hydrogenases, nitrogenases, CO dehydrogenases, etc.). Likewise, in transition metal catalyzed reactions, bimetallic catalysts can exhibit synergistic activity leading to enhanced reactivity not attainable by monometallic catalysts. Herein, we have introduced a novel strategy to manage selectivity in C–H functionalization reactions by employing bimetallic catalysts, wherein the cooperativity can be switched on or off by proper choice of main group metals to enable excellent selectivity over divergent reaction pathways. Proof-of-concept lies in the highly selective generation of either C-3 or benzylic arylation products from 2-benzylfuran derivatives. A key conceptual advance of this chemistry is the demonstration that the regioselectivity of reductive elimination can be controlled within a single ligand framework simply by employing different auxiliary metals. Our approach can be compared to traditional approaches, wherein selectivity is determined in the C–H bond cleavage step.

We have presented computational and circumstantial experimental evidence supporting the idea that the bimetallic (M~NIXANTPHOS)Pd-based catalyst system can impact the equilibrium of palladium-bound benzylic and C-3 isomers (**III** and **IV** in Figure 4) through secondary coordination sphere effects. The situation of the anionic charge on the NIXANTPHOS backbone places K^+ in an advantageous position for binding the benzylic arene ring when Pd is coordinated to the C-3 carbon of the furan (**IV**). In the absence of a suitable main group cation to bind the benzylic π-system (Li, Na or K•18-crown-6), the furanyl ligand preferentially binds to the palladium through the benzylic carbon (**III**) and leads to benzylic arylation products. We anticipate that the features of the bimetallic support scaffold of the NIXANTPHOS ligand will lead to a general design feature to control reactivity and selectivity and will inspire the synthesis and application of new classes of bimetallic catalysts.

4. EXPERIMENTAL SECTION

Representative procedures are described herein. Full experimental details and characterization of all compounds are provided in the Supporting Information.

4.1. General Methods. All reactions were performed under nitrogen using oven-dried glassware and standard Schlenk or vacuum line techniques. Air- and moisture-sensitive solutions were handled under nitrogen and transferred via syringe. Anhydrous CPME and dioxane were purchased from Sigma-Aldrich and used as solvent without further purification. Unless otherwise stated, reagents were commercially available and used as purchased without further purification. Chemicals were obtained from Sigma-Aldrich, Acros, TCI America or Alfa Aesar, and solvents were purchased from Fisher Scientific. The progress of the reactions was monitored by thin-layer chromatography using Whatman Partisil K6F 250 μm precoated 60 Å silica gel plates and visualized by short-wavelength ultraviolet light as well as by treatment with ceric ammonium molybdate (CAM) stain or iodine. Silica gel (230–400 mesh, Silicycle) was used for flash chromatography. The ^{1}H NMR and ^{13}C{^{1}H} NMR spectra were obtained using a Brüker AM-500 Fourier-transform NMR spectrometer at 500 and 125 MHz, respectively. Chemical shifts are reported in units of parts per million (ppm) downfield from tetramethylsilane (TMS), and all coupling constants are reported in hertz. The infrared spectra were obtained with KBr plates using a Perkin-Elmer Spectrum 100 Series FTIR spectrometer. High-resolution mass spectrometry (HRMS) data were obtained on a Waters LC–TOF mass spectrometer (model LCT-XE Premier) using chemical ionization (CI) or electrospray ionization (ESI) in positive or negative mode, depending on the analyte. Melting points were determined on a Unimelt Thomas–Hoover melting point apparatus and are uncorrected.

4.2. General Procedure A. Pd-Catalyzed C3 Arylation of Furans. An oven-dried 10 mL reaction vial equipped with a stir bar was charged with $KN(SiMe_3)_2$ (49.9 mg, 0.25 mmol, 2.5 equiv) under a nitrogen atmosphere. A solution (from a stock solution) of $Pd(OAc)_2$ (1.12 mg, 0.0050 mmol, 5 mol %) and NiXantphos (4.14 mg, 0.0075 mmol, 7.5 mol %) in 1 mL of dry dioxane was taken up by syringe and added to the reaction vial. After stirring for 5 min at 24 °C, 2-benzylfuran (18.1 μL, 0.12 mmol, 1.2 equiv) was added to the reaction mixture followed by 1-bromo-4-*tert*-butylbenzene (17.3 μL, 0.1 mmol, 1 equiv). Note that the aryl bromide in a solid form was added to the reaction vial prior to $KN(SiMe_3)_2$. The reaction mixture was stirred for 12 h at 24 °C, quenched with three drops of H_2O, diluted with 3 mL of ethyl acetate, and filtered over a pad of $MgSO_4$ and silica. The pad was rinsed with additional ethyl acetate, and the solution was concentrated in vacuo. The crude material was loaded onto a silica gel column and purified by flash chromatography.

4.3. General Procedure B. Pd-Catalyzed Benzylic Arylation of Furans. An oven-dried 10 mL reaction vial equipped with a stir bar was charged with $LiN(SiMe_3)_2$ (41.8 mg, 0.25 mmol, 2.5 equiv) and 12-crown-4 (80.9 μL, 0.5 mmol, 5 equiv) under a nitrogen atmosphere. A solution (from a stock solution) of $Pd(OAc)_2$ (1.12 mg, 0.0050 mmol, 5 mol %) and NiXantphos (4.14 mg, 0.0075 mmol, 7.5 mol %) in 1 mL of dry dioxane was taken up by syringe and added to the reaction vial. After stirring for 5 min at 24 °C, 2-benzylfuran (18.1 μL, 0.12 mmol, 1.2 equiv) was added to the reaction mixture followed by 1-bromo-4-*tert*-butylbenzene (17.3 μL, 0.1 mmol, 1 equiv). Note that the aryl bromide in a solid form was added to the reaction vial prior to $LiN(SiMe_3)_2$. The reaction mixture was stirred for 12 h at 24 °C, quenched with three drops of H_2O, diluted with 3 mL of ethyl acetate, and filtered over a pad of $MgSO_4$ and silica. The pad was rinsed with additional ethyl acetate, and the solution was concentrated in vacuo. The crude material was loaded onto a silica gel column and purified by flash chromatography.

ASSOCIATED CONTENT

Supporting Information. Procedures, full characterization of new compounds, and DFT geometry optimization calculations. This material is available free of charge via the Internet at http://pubs. acs.org.

AUTHOR INFORMATION

Corresponding Author

pwalsh@sas.upenn.edu, tomson@sas.upenn.edu

ACKNOWLEDGMENTS

Financial support for this work was provided by NIH/NIGMS (GM 104349). NT acknowledges Mahidol University (Thailand) and Feng Gao thanks the China Scholarship Counsel for fellowships.

REFERENCES

(1) Davies, I. W.; Welch, C. J. *Science* **2009**, *325*, 701.

(2) Colby, D. A.; Bergman, R. G.; Ellman, J. A. *Chem. Rev.* **2010**, *110*, 624.

(3) Lyons, T. W.; Sanford, M. S. *Chem. Rev.* **2010**, *110*, 1147.

(4) Yeung, C. S.; Dong, V. M. *Chem. Rev.* **2011**, *111*, 1215.

(5) Mkhalid, I. A. I.; Barnard, J. H.; Marder, T. B.; Murphy, J. M.; Hartwig, J. F. *Chem. Rev.* **2010**, *110*, 890.

(6) Daugulis, O.; Do, H.-Q.; Shabashov, D. *Acc. Chem. Res.* **2009**, *42*, 1074.

(7) Magano, J.; Dunetz, J. R. *Chem. Rev.* **2011**, *111*, 2177.

(8) Bryan, M. C.; Dillon, B.; Hamann, L. G.; Hughes, G. J.; Kopach, M. E.; Peterson, E.A.; Pourashraf, M.; Raheem, I.; Richardson, P.; Richter, D.; Sneddon, H. F. *J. Med. Chem.* **2013**, *56*, 6007.

(9) Ritchie, T. J.; Macdonald, S. J. F.; Young, R. J.; Pickett, S. D. *Drug Discov. Today* **2011**, *16*, 164.

(10) Liégault, B.; Petrov, I.; Gorelsky, S. I.; Fagnou, K. *J. Org. Chem.* **2010**, *75*, 1047.

(11) Engle, K. M.; Mei, T.-S.; Wasa, M.; Yu, J.-Q. *Acc. Chem. Res.* **2011**, *45*, 788.

(12) Liu, Y.-J.; Xu, H.; Kong, W.-J.; Shang, M.; Dai, H.-X.; Yu, J.-Q. *Nature* **2014**, *515*, 389.

(13) Leow, D.; Li, G.; Mei, T.-S.; Yu, J.-Q. *Nature* **2012**, *486*, 518.

(14) Roosen, P. C.; Kallepalli, V. A.; Chattopadhyay, B.; Singleton, D. A.; Maleczka, R. E., Jr.; Smith, M. R., III. *J. Am. Chem. Soc.* **2012**, *134*, 11350.

(15) Zhang, J.; Bellomo, A.; Trongsiriwat, N.; Jia, T.; Carroll, P. J.; Dreher, S. D.; Tudge, M. T.; Yin, H.; Robinson, J. R.; Schelter, E. J.; Walsh, P. J. *J. Am. Chem. Soc.* **2014**, *136*, 6276.

(16) van der Veen, L. A.; Keeven, P. H.; Schoemaker, G. C.; Reek, J. N. H.; Kamer, P. C. J.; van Leeuwen, P. W. N. M.; Lutz, M.; Spek, A. L. *Organometallics* **2000**, *19*, 872.

(17) Shibasaki, M.; Kanai, M.; Matsunaga, S.; Kumagai, N. *Acc. Chem. Res.* **2009**, *42*, 1117.

(18) Buchwalter, P.; Rosé, J.; Braunstein, P. *Chem. Rev.* **2015**, *115*, 28.

(19) (a) Sperry, J. B.; Wright, D. L. *Curr. Opin. Drug Discovery Dev.* **2005**, *8*, 723. (b) Li, J. J. *Heterocyclic Chemistry in Drug Discovery*; John Wiley & Sons, 2013.

(20) Palladium-catalyzed bisarylation of 3-alkylbenzofurans with aryl iodides: Cho, B. S.; Chung, Y. K. *Chem. Commun.* **2015**, *51*, 14543.

(21) Bordwell, F. G. *Acc. Chem. Res.* **1988**, *21*, 456.

(22) Bellomo, A.; Zhang, J.; Trongsiriwat, N.; Walsh, P. J. *Chem. Sci.* **2013**, *4*, 849.

(23) Zhang, J.; Bellomo, A.; Creamer, A. D.; Dreher, S. D.; Walsh, P. J. *J. Am. Chem. Soc.* **2012**, *134*, 13765.

(24) Hussain, N.; Frensch, G.; Zhang, J.; Walsh, P. J. *Angew. Chem., Int. Ed.* **2014**, *53*, 3693.

(25) Kumpf, R. A.; Dougherty, D. A. *Science* **1993**, *261*, 1708.

(26) Cordero, B.; Gómez, V.; Platero-Prats, A. E.; Revés, M.; Echeverría, J.; Cremades, E.; Barragán, F.; Alvarez, S. *Dalton Trans.* **2008**, 2832.

(27) Dougherty, D. A. *Acc. Chem. Res.* **2012**, *46*, 885.

(28) Meyer, E. A.; Castellano, R. K.; Diederich, F. *Angew. Chem., Int. Ed.* **2003**, *42*, 1210.

(29) KO^tBu was used as base because $KN(SiMe_3)_2$ caused decomposition of the substrate.

(30) Pan, X.; Yang, X.; Chen, L.; Wu, J.; Tang, N. *Inorg. Chem. Commun.* **2010**, *13*, 919.

(31) Mansell, S. M.; Kaltsoyannis, N.; Arnold, P. L. *J. Am. Chem. Soc.* **2011**, *133*, 9036.

(32) Akagi, F.; Matsuo, T.; Kawaguchi, H. *Angew. Chem., Int. Ed.* **2007**, *46*, 8778.

(33) Hsu, Y.-L.; Liang, L.-C. *Organometallics* **2010**, *29*, 6201.

(34) Sarazin, Y.; Roşca, D.; Poirier, V.; Roisnel, T.; Silvestru, A.; Maron, L.; Carpentier, J.-F. *Organometallics* **2010**, *29*, 6569.

TOC

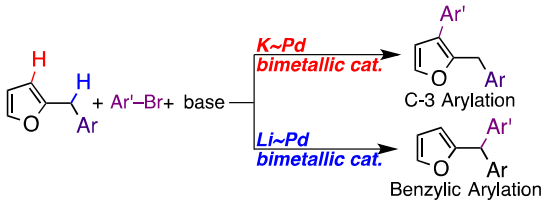
H
H
O
Ar
+ Ar'–Br+ base
K~Pd
bimetallic cat.
Li~Pd
bimetallic cat.
Ar'
O
Ar
C-3 Arylation
Ar'
O
Ar
Benzylic Arylation